Dhofar 025, 301, 304, 308

Anorthositic regolith breccia

751, 9, 10, 2 g

Figure 1: Photo of Dhofar 025 with a 1 cm cube for scale (photo from R. Korotev).

Introduction

Dhofar 025 (Fig. 1) was found in the Dhofar region of Oman (Figs. 2 and 3) in January, 2000 (Grossman et al., 2000). The 751 g brownish gray stone lacks fusion crust, and has terrestrial weathering in cracks such as akaganeite (FeOOH), calcite, celestite, barite, and gypsum (Fig. 4). Smaller additional stones Dhofar 301, 304 and 308 were found in April 2001, and are paired on the basis of their location of find, textures and chemical compositions.

Petrography and mineralogy

Dhofar 025 is a regolith breccia consisting of many mineral fragments and lithic clasts in a glassy matrix. Clasts include anorthositic troctolite and troctolite, as well as granulites (Grossman et al., 2000). Plagioclase feldspar has a narrow compositional range between An_{94} and An_{98}. Mosts clasts are impact melt rocks with microporphyritic textures that include plagioclase crystals within a mafic mineral and feldspar matrix (e.g., Fig. 5,6). Relict rocks and minerals grains are often embayed and perhaps partially resorbed by the surrounding melt (Fig. 5; Cahill et al., 2001, 2004). Mafic minerals are minor in general and consist of olivine (Fig. 7; Fo_{60-88}), orthopyroxene (Fig. 7; Mg# ~ 0.75), pigeonite (Fig. 7; Mg# 0.65 to 0.69), and augite (Fig. 7; Mg# 0.66 to 0.80). As with other lunar feldspathic meteorites, Dhofar 025 olivine, pyroxene, and plagioclase clast compositons span the gap between the High Mg suite (HMS) and ferroan anorthosites (FAN) (Fig. 8). Accessory minerals include spinel, ilmenite, FeNi metal, troilite, and silica.

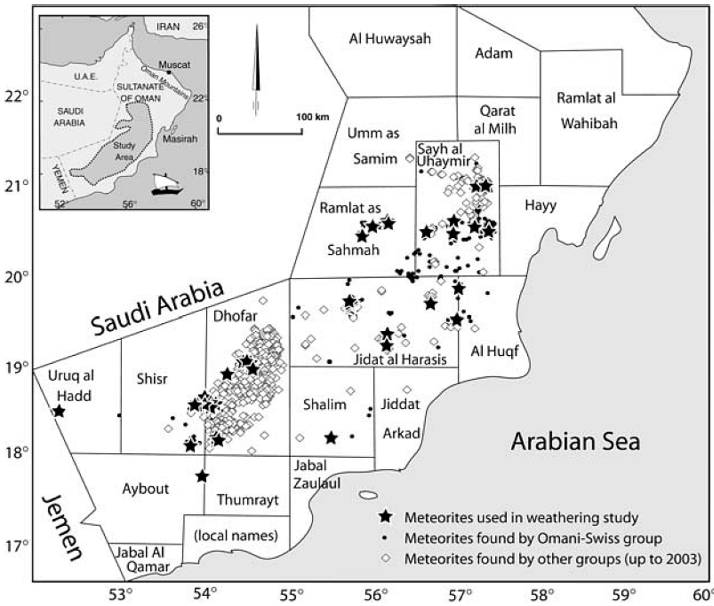

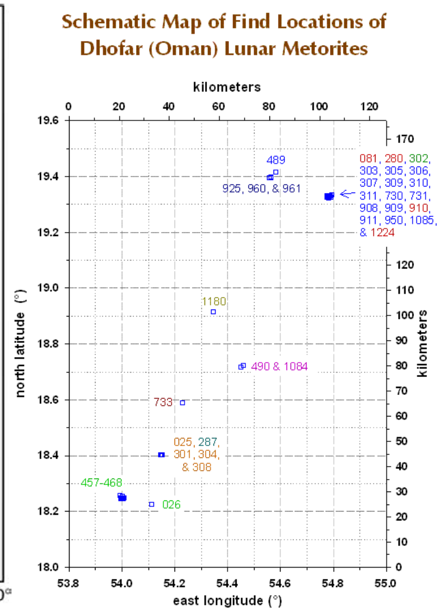

Figure 2: Map showing location of regions within Oman where meteorites have been recovered, such as Dhofar.

Figure 3: More detailed locations of the Dhofar meteorites, including Dho 025, 310, 304, and 308 (shown in orange in lower left).

Figure 4: Photo of a slab of Dhofar 025, illustrating the pink diffuse nature of the clasts as well as the fractures filled with terrestrial alteration (celestite or calcite). Scale bar at top is in mm.

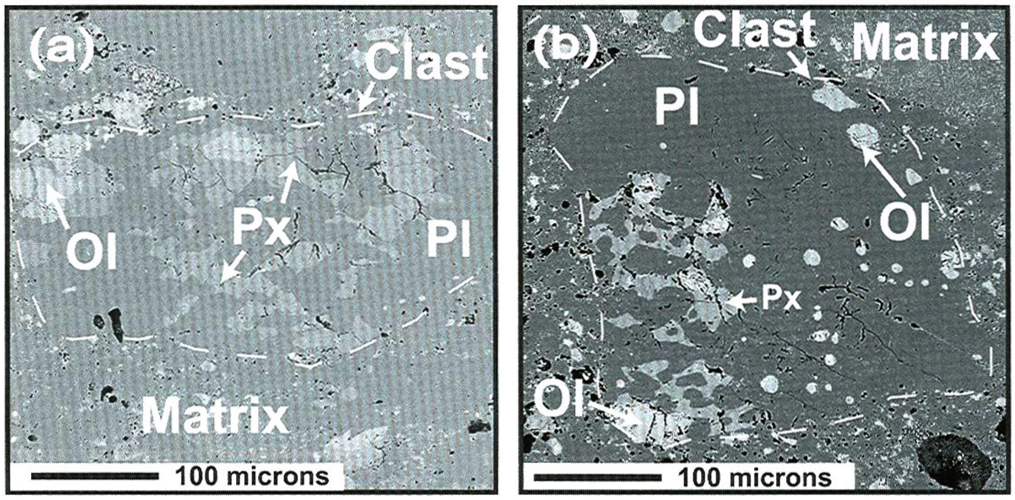

Figure 5: Two backscattered electron images of lithic clasts from Dhofar 025, illustrating embayed mafic minerals resulting from interaction with impact melt. The clasts are surrounded by a fine-grained and glassy matrix (from Cahill et al., 2004).

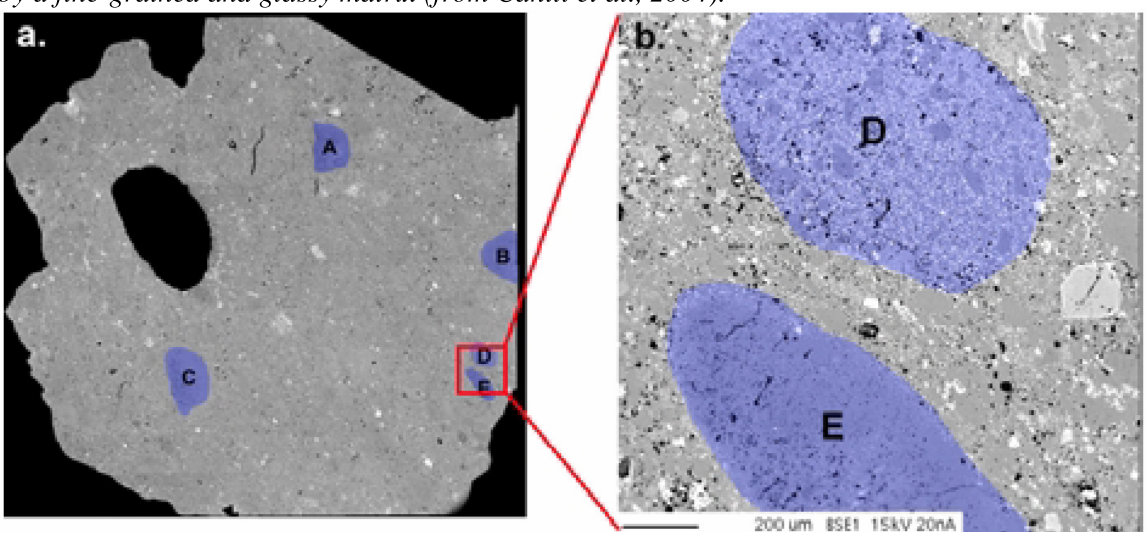

Figure 6: Back scattered electron image of the Dhofar 025 illustrating the textures in this breccia, as well as highlighting (in blue) several of the clasts analyzed by Cohen et al. (2001).

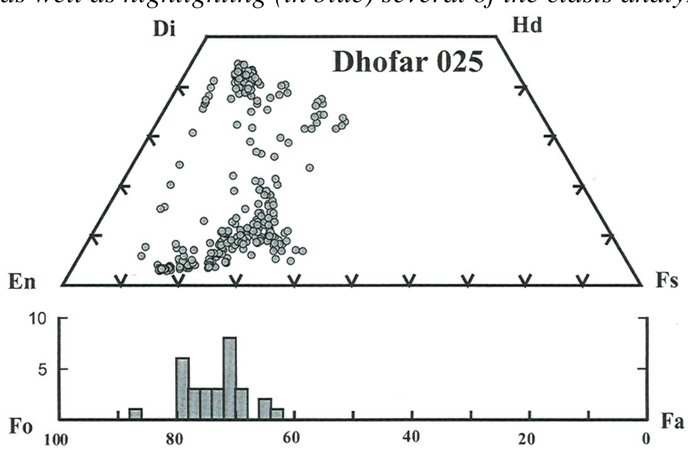

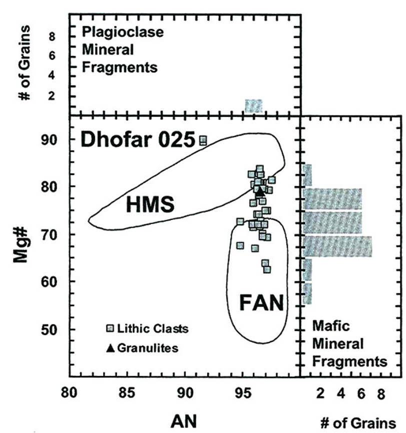

Figure 7: Pyroxene and olivine compositions from clasts in Dhofar 025 (from Cahill et al., 2004).
Figure 8: Mg# vs. An content of pyroxene and olivine from clasts in Dhofar 025 (from Cahill et al., 2004).

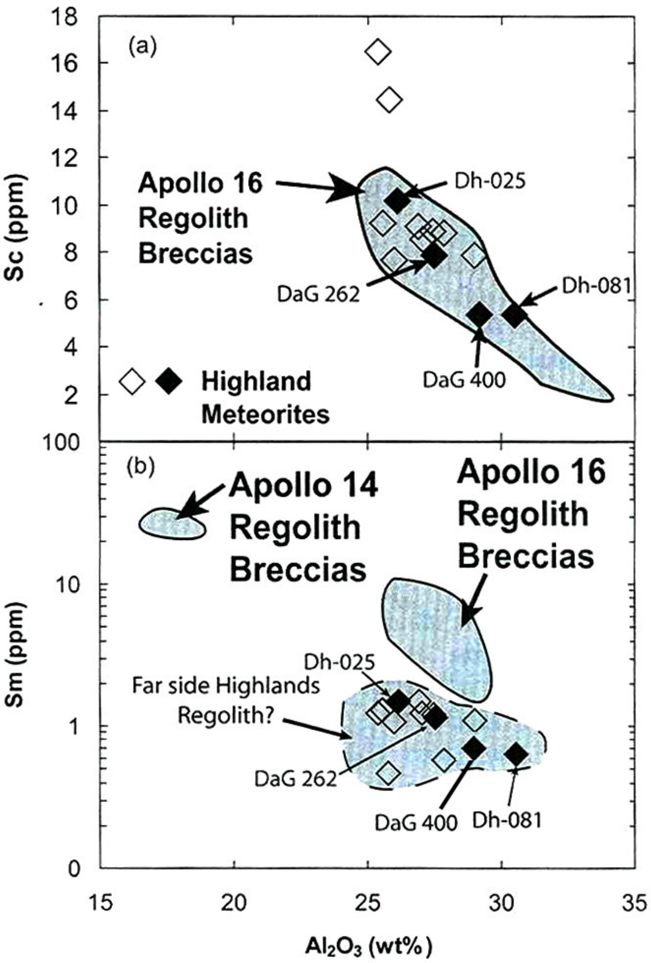

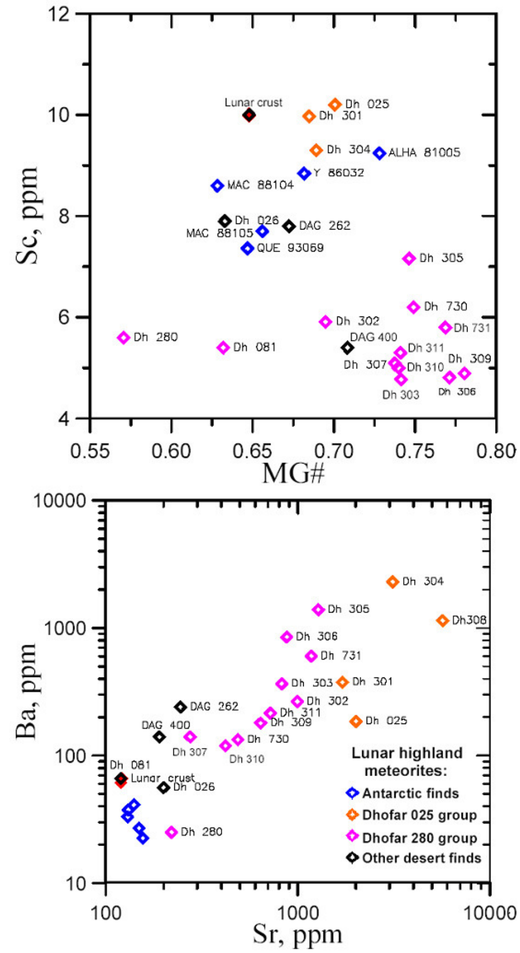

Figure 9: Sc and Sm (ppm) vs. Al_2O_3 for some lunar highlands meteorites including Dhofar 025 (from Cahill et al., 2004).

Figure 10: .Sc vs. Mg# and Ba vs. Sr for some of the Dhofar meteorites including Dhofar 025 (from Nazarov et al. (2004)

Chemistry

Dhofar 025 and its pairs have compositional features that make lunar feldspathic meteorites distinct from Apollo samples - they have high Al_2O_3 (~ 27 wt%) and low FeO (~5 wt%). They have similar Sc and siderophile elements such as Ir, compared to Apollo 14 and 16 breccias, but lower Sm, Th, and Na (Figs. 9 and 10; Warren et al., 2005; Cahill et al., 2004; Korotev et al., 2003). Rare earth elements (REE) are as high as QUE 93069 and Dhofar 026 - higher than many lunar feldspathic meteorites (Fig. 11). Also, elements such as Ba and Sr are elevated above values for other Antarctic feldspathic meteorites, most likely from terrestrial alteration (Nazarov et al., 2004; Floss and Crozaz, 2001; Korotev et al., 2003; Bischoff et al., 1998).

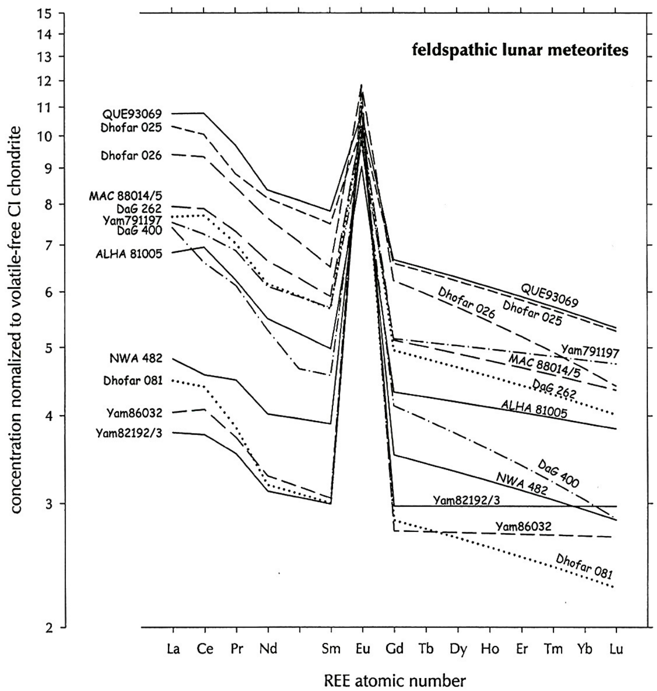

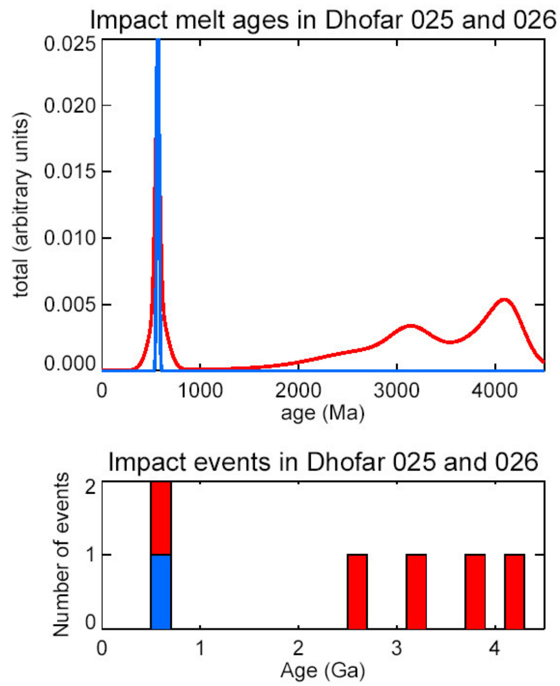

Figure 11: REE concentrations for Dho 025 compared to those for other lunar feldspathic meteorites (from Korotev et al., 2003).
Figure 12: Summary of Ar-Ar dating of individual impact melt clasts in Dhofar 025 and 026 (from Cohen et al. (2002).

Radiogenic age dating

Two kinds of chronologic studies have been completed on Dhofar 025. Cohen et al. (2002) have applied the laser fusion techniques to 15 individual clasts from Dho 025 and found age clustering at 500 Ma, 3.1 Ga and 4.0 Ga (Fig. 12). These three groupings may represent individual impact events. In another study, U-Pb dating of zircons using an ion microprobe was undertaken by Leonteva et al. (2005). Results from that study indicate a possible age of 4360 Ma, abut with a disturbance at 2000 Ma or younger (Fig. 13). The latter age may represent the age of brecciation or a young impact event.

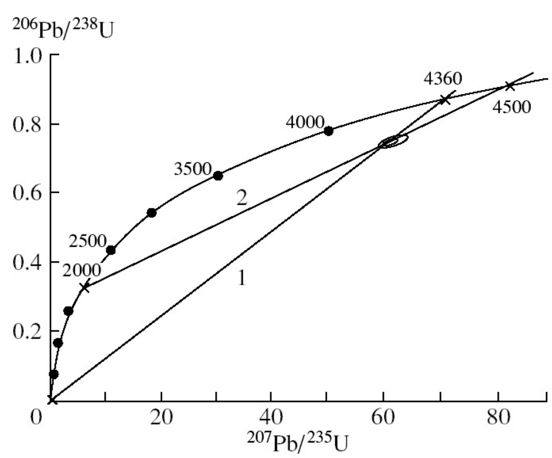

Figure 13: Mineral isochron for Dho 025 for the U-Pb system in zircons (from Leonteva et al., 2005).

Cosmogenic isotopes and exposure ages

Studies of noble gases and cosmic ray exposure ages have yielded the oldest terrestrial exposure age of all lunar meteorites – 500 to 600 Ka (Nishiizumi et al. (2001, 2004). The light noble gases, He, Ne and Ar, yield an exposure age of > 10 Ma (Lorenzetti et al., 2005), in agreement with the 13-20 Ma result of Nishiizumi et al. (2001, 2004). These results indicate the Dhofar 025 has the oldest ejection age and transit time.

Table 1: Chemical composition of Dho 025

					Dho 308	Dho 301	Dho 304
reference	1	2	3	3	4	4	4
weight	104	1000	73	31.5			
method	e	b,e,g	e	d	e	a,e,g	a,e,g
SiO_2 %	44.71	43.9		44.2		44.1	45
TiO_2	0.30	0.3		0.29		0.36	0.34
Al_2O_3	26.63	26.1		26.9		28.6	25.3
FeO	4.82	4.98	4.76	4.9	5.41	4.27	5.71
MnO	0.07	0.08		0.05		0.07	0.12
MgO	6.37	6.53		7.1		4.83	7.09
CaO	15.67	16.1	15.5	16.2		16.5	14.8
Na_2O	0.34	0.282	0.345	0.35	0.47	0.41	0.37
K_2O	0.05	0.07	0.09	0.039		0.04	0.04
P_2O_5		0.08		0.06		0.07	0.07
S %							
sum							
Sc ppm	9.8	10.2	9.82		10.3	9.97	9.3
V	23						
Cr	810	674	766	753	632	651	591
Co	15.3	16.5	15.39		22	13.6	18.1
Ni	113	200	127		130	260	200
Cu							
Zn							
Ga	3.1	3.1					
Ge							
As	0.17		0.19				
Se							
Rb			<5				
Sr	1410	2010	2090		5680	1710	3120
Y							
Zr	42	62	52		115	27	65
Nb							
Mo							
Ru							
Rh							
Pd ppb							
Ag ppb							
Cd ppb							

In ppb							
Sn ppb							
Sb ppb	22		35				
Te ppb							
Cs ppm	<0.02	0.55	<0.12				
Ba	110	130	110		1140	375	2302
La	3	3.6	3.27		4	3.68	4.1
Ce	7.4	8.6	8.71		9.7	8.4	9
Pr							
Nd	4.7	5.2	5.1		6	4.6	4.7
Sm	1.35	1.5	1.646		1.8	1.28	1.3
Eu	0.74	1.3	0.819		1	0.74	0.74
Gd							
Tb	0.27	0.35	0.337		0.39	0.24	0.3
Dy	1.6						
Ho	0.38	0.44					
Er							
Tm							
Yb	1.07	1.2	1.28		1.2	0.63	1.1
Lu	0.16	0.21	0.179		0.18	0.099	0.18
Hf	0.98	1.3	1.26		1.4	0.79	0.79
Ta	0.13	<0.3	0.134		0.44		
W ppb			<700				
Re ppb		<20					
Os ppb		<300					
Ir ppb	4.5	7.2	3.7		26	5.6	20
Pt ppb							
Au ppb	4.9	3	7.4		9	4	13
Th ppm	0.46	0.8	0.525		1.7	0.66	0.5
U ppm	0.19	0.27	0.2		1		

technique (a) ICP-AES, (b) ICP-MS, (c) IDMS, (d) FB-EMPA, (e) INAA, (f) RNAA, (g) XRF

Table 1b. Light and/or volatile elements for Dho 025

Li ppm	
Be	
C	
S	
F ppm	
Cl	
Br	1.11
I	
Pb ppm	
Hg ppb	
Tl	
Bi	

References: 1) Warren et al. (2005); 2) Cahill et al. (2004) and Demidova et al. (2007); 3) Korotev et al. (2003); 4) Demidova et al. (2007)